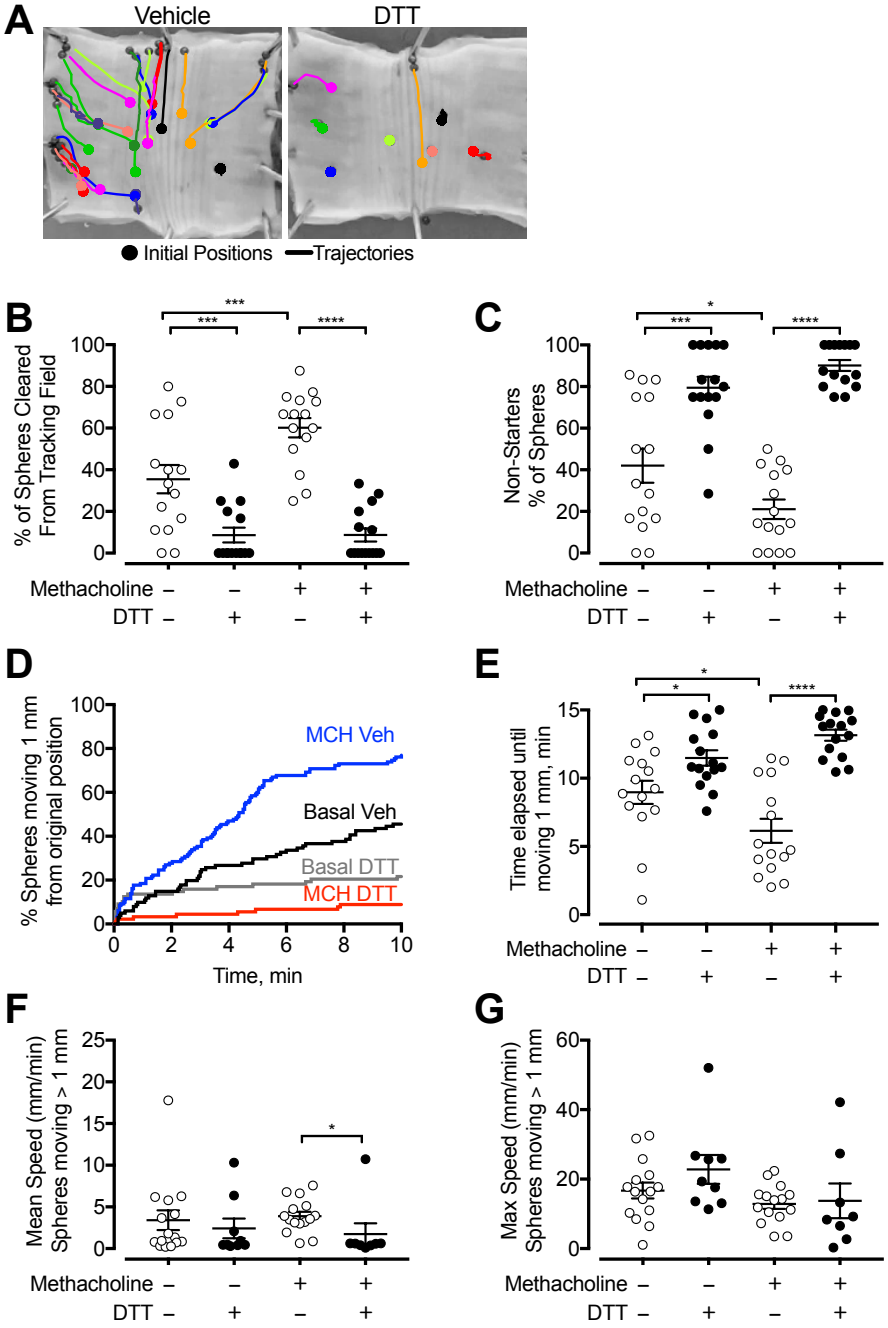

Supplemental Figure 1. DTT impairs transport of metallic spheres *ex vivo*.

A. In an example experiment, several metallic spheres were transported in the presence of vehicle, but few spheres were transported in the presence of 1 mM DTT. Dots represent original positions and lines

represent the subsequent trajectory. Spheres are depicted with different colors. Data presented correspond to Supplemental Video 6.

B. DTT significantly decreased the percentage of spheres that were cleared from the tracking field under basal and methacholine stimulated conditions. Control data are identical to Figure 3B. N = 15 pigs per group.

C. DTT significantly increased the percentage of spheres that were non-starters (i.e. spheres that move ≤ 1 mm) under basal and methacholine stimulated conditions. Spheres were tracked for at least 10 minutes. Control data are identical to Figure 4B. N = 15 pigs per group.

D-E. DTT delayed the initiation of movement of spheres. **D.** The percentage of spheres moving > 1 mm from their origin position is shown as a function of time. Data are inclusive of all 15 experiments. Between 88 and 130 spheres were tracked per condition. Control data are identical to those shown in Fig 4C. **E.** Data are the mean time that spheres remained within 1 mm of their origin. Control data are identical to those shown in Fig 4D. For **B-E**, * $P < 0.05$, ** $P < 0.01$, *** $P < 0.001$, **** $P < 0.0001$ by 2-way repeated measures ANOVA with Holm-Sidak's post-hoc multiple comparisons test. Each data point is from a different pig, lines and error bars represent mean ± SEM. Some error bars are hidden by symbols.

F-G. Mean (**F**) and maximum (**G**) speed of Ta spheres after moving 1 mm in the presence or absence of DTT. N = 8-15 pigs per group. Note that N was less than 15 for some groups because in some experiments including DTT, no spheres moved more than 1 mm. * $P < 0.05$ by Kruskal-Wallis test with Dunn's post-hoc multiple comparison test. For maximum speed, there were no differences between groups. Control data are identical to those shown in Fig 4E-F.

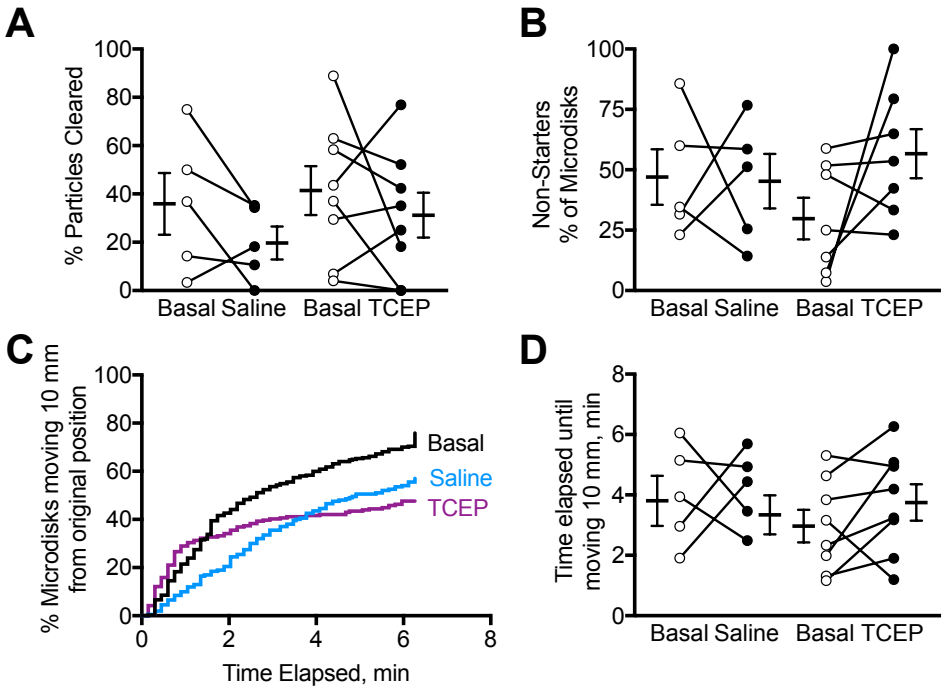

Supplemental Figure 2. Effect of inhaled TCEP on in vivo mucociliary transport in the absence of methacholine stimulation.

Data are from *in vivo* tracking of tantalum microdisks using CT-based assay. Data were obtained under basal conditions or after administration of aerosolized vehicle or aerosolized TCEP. **A.** Percentage of microdisks that were cleared from the lungs during the 6.3 min tracking period. **B.** Percentage of microdisks that were non-starters. **E.** Percentage of microdisks moving > 10 mm from original position as a function of time. Data are pooled from multiple experiments, with 200 - 317 microdisks tracked per condition. Conditions are basal (black), saline vehicle (light blue), and TCEP (purple). **D.** Time elapsed before microdisks moved > 10 mm from original position. Each set of data points and connecting lines is from a different pig.

Video 1. Mucus strands extrude from submucosal gland ducts. A mucus strand labeled with red fluorescent nanospheres was visualized as it emerged from a submucosal gland duct. The ciliated surface epithelium is shown in gray. The strand twisted as it extruded from the duct. The strand was then released from the duct. The video is shown at 10 x speed (original duration 1:08).

Video 2. Dynamic movements of mucus strands, including extending and snapping back. Mucus strands were labeled with red fluorescent nanospheres and their movement was monitored over 6 seconds using confocal microscopy. The left strand extended in the direction of ciliary flow. The right strand broke and abruptly snapped back between 2.5 and 2.7 seconds. The video is shown in real time.

Video 3. Mobile strands of mucus can form new connections with stationary mucus stands. A mucus strand emerged from a SMG duct near a second strand originating below the field of view. A moving strand entered the field of view. The moving strand then formed a new connection with the two previously existing stationary strands. The strand subsequently released from the SMG duct. The video is shown in real time.

Video 4. Networks of mucus strands are transported over the epithelial surface in the absence of methacholine. 40 nm green fluorescent nanospheres were used to label mucus strands. A network of mucus strands entered the field and flowed over the airway surface. This network contained strands that flowed perpendicular to the axis of ciliary transport (squeegee strands). These strands were linked to other strands that moved parallel to the direction of flow. The video is shown in real time.

Video 5. Networks of mucus strands are transported over the epithelial surface in the presence of methacholine. In the presence of methacholine stimulation, networks of mucus strands moved over the airway surface. The video is shown in real time.

Video 6. Impaired transport of steel spheres in the presence of reducing agent. Matched trachea segments were dissected from a non-CF piglet and submerged in Krebs buffered saline at 37 °C in the presence or absence of 1 mM DTT. Steel spheres were applied to the mucosal surface of each segment. In both specimens, some spheres lagged prior to movement. In the presence of DTT, fewer particles moved > 1 mm from the original position. Video is 44 x actual speed (original duration 16:00).

Video 7. Mucus strands facilitate transport of a Ta sphere after methacholine stimulation. A Ta sphere was added to the surface of a pig trachea following methacholine stimulation. Prior to strand binding, the sphere rolled in place. Strands labeled with green fluorescent nanospheres struck the sphere, reoriented it, and dragged it in the direction of ciliary transport until the sphere reached the edge of the tissue. Video is 64 x actual speed (original duration 7:08).

Video 8. A mucus strand network initiates the transport of a steel sphere after methacholine stimulation. A steel sphere was stationary on the surface of a pig trachea explant following methacholine stimulation. A complex of strands, made visible by addition of red fluorescent nanospheres, struck the sphere. After the strands collided with the sphere, the sphere was reoriented. Mucus strands extended in the direction of ciliary transport. Individual strands tightened and pulled the sphere forward to the rostral tissue edge. Video is 14 x actual speed (original duration 1:10).

Video 9. Mucus fragments attach to a Ta sphere after methacholine stimulation in the presence of TCEP, but do not initiate movement of the sphere. A Ta sphere was added to pig trachea following methacholine stimulation in the presence of 1 mM TCEP. The sphere rolled in place. Strand fragments labeled with green fluorescent nanospheres struck the sphere. However, the sphere continued to roll in place and accumulate mucus fragments without being transported to the tissue edges. Video is 64 x actual speed (original duration 16:01).

Video 10. Mucus fragments attach to a Ta sphere after methacholine stimulation in the presence of DTT, but do not initiate movement of the sphere. A Ta sphere was added to pig trachea following methacholine stimulation in the presence of 1 mM DTT. There were many small mucus fragments, which are labeled with green nanospheres. Some mucus fragments attached to the Ta sphere. Despite attachment of these fragments, the sphere continued to roll in place without being transported to the tissue edges. Video is 64 x actual speed (original duration 17:26).

Video 11. Transport of microdisks in untreated pig airways. The airway tree of a pig is shown in gray. Microdisks, each represented by a different colored diamond, were insufflated into the airways and tracked by sequential CT scanning. Some microdisks remained near their origin throughout the tracking period. Other microdisks were transported past the stationary microdisks with variable delay time prior to transport. Video is 85 x actual speed (original duration 6.3 min).

Video 12. Transport of microdisks in a pig receiving IV methacholine and inhaled vehicle. The airway tree of a pig that received IV methacholine and inhaled vehicle is shown in gray. Microdisks, each represented with a colored diamond, were insufflated into the airways and tracked by sequential CT scanning. Most of the microdisks were transported from their original position. There was minimal delay before the microdisks started moving. After the microdisks started moving, they travelled rapidly toward the larynx. Video is 85 x actual speed (original duration 6.3 min).

Video 13. Transport of microdisks in a pig receiving IV methacholine and inhaled TCEP. The airway tree of a pig that received IV methacholine and inhaled TCEP is shown in gray. Microdisks, each represented with a colored diamond, were insufflated into the airways and tracked by sequential CT scanning. Many microdisks remained near their original position during the tracking. Among the microdisks that moved, the speed was greater than the baseline condition. Video is 85 x actual speed (original duration 6.3 min).